Applied and Environmental Microbiology, June 2007, p. 3677–3683 Vol. 73, No. 11
0099-2240/07/$08.00+0 doi:10.1128/AEM.00428-07

Sonoporation Is an Efficient Tool for Intracellular Fluorescent Dextran Delivery and One-Step Double-Crossover Mutant Construction in *Fusobacterium nucleatum*▽

Yiping W. Han,[1,2]* Akihiko Ikegami,[1] Peter Chung,[3] Lei Zhang,[1] and Cheri X. Deng[4]

Department of Biological Sciences, School of Dental Medicine,[1] Department of Pathology, School of Medicine,[2] Department of Chemistry, School of Arts and Sciences,[3] and Department of Biomedical Engineering, School of Engineering,[4] Case Western Reserve University, Cleveland, Ohio 44106-4905

Received 23 February 2007/Accepted 8 April 2007

Studies of microorganisms are often hindered by a lack of effective genetic tools. One such example is *Fusobacterium nucleatum*, a gram-negative anaerobe associated with various human infections, including those causing periodontal disease and preterm birth. The first double-crossover allelic-exchange mutant in *F. nucleatum* was recently constructed using sonoporation, a novel ultrasound-mediated intracellular delivery method, demonstrating potential for bacterial gene transfection. To better unveil its mechanism, the current study examines the factors affecting the outcome of sonoporation. Delivery of Texas Red-conjugated dextran into *F. nucleatum* by sonoporation was at least twice as efficient as that by electroporation, and sonoporation was nonbactericidal, unlike electroporation. The delivery efficiency was affected by the acoustic pressure amplitude, the duty cycle, and the quantity of microbubbles used to initiate cavitation but not by the pulse repetition frequency of ultrasound application. To examine the involvement of homologous recombination in sonoporation-mediated mutant construction, the highly conserved *recA* gene, which carried most of the consensus residues, including the P loop, was identified in *F. nucleatum*, and a double-crossover *recA* mutant of *F. nucleatum* 12230, US1610, was constructed by sonoporation. The mutant exhibited increased sensitivity to UV exposure compared with that of the wild type, indicating that the RecA function in *F. nucleatum* was conserved. Interestingly, US1610 was also sensitive to ultrasound treatment, suggesting the likely involvement of RecA in postsonoporation repair and survival. Since sonoporation has consistently generated one-step double-crossover mutants in *F. nucleatum* by use of intact suicide plasmids, this technology may be developed into an efficient tool for streamlining mutant construction in bacteria.

Fusobacterium nucleatum is a gram-negative anaerobe ubiquitous to the oral cavity and associated with various common human infections incurring high medical costs and risks to patients, including infections causing periodontal disease and preterm birth (16). Studies of this opportunistic human pathogen have been hindered by a lack of effective genetic tools. Genetic manipulation of *F. nucleatum* has been difficult, presumably due in part to its diversified restriction endonuclease systems, which differ between strains and cleave DNA irrespective of the extent of methylation (11). Although mobile genetic elements were identified in *F. nucleatum* nearly a decade ago (13), and several shuttle plasmids have been constructed and delivered into two strains, *F. nucleatum* ATCC 10953 and ATCC 23726, by electroporation (5, 10), no genetic work had been successful in *F. nucleatum* 12230, a working strain in our laboratory known to be refractory to such manipulations. Recently, a novel FadA adhesin that encodes a small open reading frame of 387 bp was identified in *F. nucleatum* 12230. The small open reading frame rendered construction of the allelic exchange mutant difficult. Unsuccessful with electroporation and conjugation, we established a sonoporation technique and constructed US1 (Δ*fadA*::*ermF-ermAM*), the first allelic exchange mutant in *F. nucleatum* 12230, using ultrasound (US) application at a 1-MHz center frequency (7).

US is a mechanical wave energy generated in a medium as oscillating pressure in space and time at frequencies above 20 kHz, beyond the audible range. US exposure generates bioeffects resulting in tissue heating, shear stress, and cavitation, which have been exploited for therapeutic applications. Particularly, cavitation, the formation and rapid collapsing of gas bubbles in the host media, has been utilized for intracellular delivery of drugs and genes. Cavitation can cause drastic local physical and chemical changes, including microstreaming, high-speed microjetting, extremely high localized temperature and pressure inside bubbles, and generation of free radicals (H^+, OH^-, O_2^-) (14, 23). If a cell is in the vicinity during these changes, the cell membrane may be damaged or disrupted locally, allowing entry of extracellular agents into the cytoplasm. This process is termed sonoporation, in recognition of its similarity to electroporation. Like electroporation, sonoporation can be classified into two categories based on its outcome: (i) reparable, or reversible, sonoporation, during which the induction of temporary pores on the cell membrane is followed by pore resealing, leading to cell survival (2), and (ii) lethal, or irreversible, sonoporation, where the cell membrane is irreversibly damaged or the cell is lysed, leading to cell death (23). Reparable sonoporation is an emerging technology for intracellular delivery of drugs, genes, and other agents for

* Corresponding author. Mailing address: Department of Biological Sciences, School of Dental Medicine, Case Western Reserve University, 10900 Euclid Avenue, Cleveland, OH 44106-4905. Phone: (216) 368-1995. Fax: (216) 368-0145. E-mail: yiping.han@case.edu.
▽ Published ahead of print on 20 April 2007.

diagnostic and/or therapeutic purposes (14) and has been increasingly used in mammalian cells and in vivo (8, 15, 17, 21, 22). To the best of our knowledge, the use of sonoporation to construct US1 was the first application of this technology to bacteria (7). Most interestingly, all transformants obtained by sonoporation were double-crossover allelic-exchange mutants, despite the fact that an intact suicide plasmid was used. Although double-crossover allelic exchange using intact suicide plasmid has been observed in gram-positive species, such as *Streptococcus* spp., such events had not been reported for gram-negative bacteria before (3, 19). Using the same suicide plasmid in numerous trials, we eventually obtained one colony each from electroporation and conjugation. Both constructs appeared to be single crossovers (unpublished results). Therefore, the one-step construction of double crossovers was not caused by the plasmid or *F. nucleatum*; rather, it is likely a unique feature of sonoporation. If this is true, sonoporation has the potential to become a powerful genetic tool for streamlining mutant construction in bacteria.

In this study, the mechanism of sonoporation in *F. nucleatum* 12230 was investigated. The effects on intracellular delivery outcome by different sonoporation parameters were tested using fluorescent dextran. A double-crossover *recA* mutant was constructed via sonoporation to assess the involvement of homologous recombination in the process. As this mutant exhibited increased sensitivities to both UV and sonoporation treatment, RecA is likely involved in reparable sonoporation in *F. nucleatum*. Thus, gene transfection by sonoporation in bacteria employs a mechanism different from that in eukaryotic cells, as RecA is unique to bacteria.

MATERIALS AND METHODS

Bacterial strains and plasmids. *F. nucleatum* strains 12230 and US1610 (*F. nucleatum* 12230 *recA*::*ermF-ermAM*) were maintained as described previously (6). *Escherichia coli* TOP10, used as a host strain for plasmid construction, was grown at 37°C in LB broth (Fisher Scientific). Plasmids pYH1377 and pYH1380 were constructed as follows. The *recA* gene of *F. nucleatum* 12230 was amplified by the oligonucleotide primers FN0546F (5′-GTTTACATGGGGATAAAGTTTGTCC-3′) and FN0548R (5′-CATCTTTAACTATATCTGCAAAACC-3′) on the basis of the genome database of *F. nucleatum* ATCC 25586 from The Institute for Genomic Research (TIGR; http://www.tigr.org). The 1.4-kb PCR product was treated with Exo/SAP-IT (USB Co., Cleveland, OH) and was sequenced at the Molecular Biotechnology Core (Lerner Research Institute, Cleveland, OH). A portion of the *recA* gene (772 bp) was amplified from *F. nucleatum* 12330 by the oligonucleotide primers *recA*F (5′-GTGAAAAAAATGGCAGCAAAG-3′) and *recA*R (5′-CTTCCTATTGGATCATCACC-3′). The amplified fragment was cloned into the pCR2.1 vector (Invitrogen, Carlsbad, CA). The resulting plasmid, pYH1377, was digested with HincII within the cloned fragment, and a 2.4-kb PvuII *ermF-ermAM* cassette from pVA2198 (4) was inserted into this site to generate pYH1380.

Delivery of fluorescent dextran into *F. nucleatum*. Log-phase *F. nucleatum* 12230 was harvested, washed, and resuspended in phosphate-buffered saline (PBS) supplemented with 0.1 mM $CaCl_2$ and 0.1 mM $MgCl_2$. The bacterial suspension, with approximately 1×10^9 CFU, was mixed with 2.5 mg/ml Texas Red-conjugated dextran (70 kDa; Invitrogen) and the contrast agent Definity (Bristol-Myers Squibb, North Billerica, MA) in an eight-well, flat-bottom immunomodule (catalog number 468667; Nalge Nunc International, Rochester, NY). Definity is an FDA-approved, commercially available US contrast agent which consists of octafluoropropane gas bubbles that are encapsulated in lipid and dispersed in solution. The mixture was subjected to US treatment as described previously (7), transferred to microcentrifuge tubes, washed four times, each followed by centrifugation at 14,000 rpm (18,000 × *g*), and resuspended in 500 μl PBS. The bacterial cells were then examined under a fluorescence microscope. The viable counts were determined by plating serial dilutions on blood agar plates. For electroporation, the same amounts of dextran and *F. nucleatum* were used under the following conditions: 20 kV/cm, 25 μF, and 200 Ω, which are optimal for fusobacteria (5).

Construction of a *recA* mutant in *F. nucleatum*. Log-phase *F. nucleatum* 12230 cultures were washed and resuspended in PBS supplemented with 0.1 mM $CaCl_2$ and 0.1 mM $MgCl_2$. Bacterial suspension was mixed with 50 μg plasmid pYH1380 and 50 μl Definity in the Nunc eight-well immunomodule as described above. The mixture was subjected to 1-MHz US treatment under 0.5 MPa for 90 seconds, with a duty cycle of 50% (7). The bacterial suspension was then plated onto Columbia blood agar plates and incubated for 24 h at 37°C under anaerobic conditions before being replicated using velvet-covered blocks onto Columbia blood agar plates containing 0.4 mg/ml clindamycin. The plates were incubated for three additional days at 37°C under anaerobic conditions. The clindamycin-resistant colonies were isolated, purified, and inoculated in Columbia broth containing 0.4 mg/ml clindamycin. The mutants were verified by PCR using the primers *recA*F and *recA*2R (5′-ATAAGTCTAGCTTGTAATCCC-3′).

UV and sonoporation sensitivity test. UV sensitivity was determined using a method modified from Liu et al. (10a). *F. nucleatum* strains were harvested and resuspended in Columbia broth to a density of 5×10^8 CFU/ml. Aliquots (10 μl) of serial dilutions were spread on Columbia blood agar plates. The plates were exposed to UV light (254 nm) in a CL-1000 UV cross-linker (UVP, Upland, CA) for the indicated periods of time, followed by anaerobic incubation at 37°C for 3 days. For the sonoporation sensitivity test, *F. nucleatum* strains were harvested and resuspended in PBS supplemented with 0.1 mM $CaCl_2$ and 0.1 mM $MgCl_2$ to a density of 1×10^{10} CFU/ml. Bacterial suspension was mixed with 50 μl Definity in the Nunc eight-well immunomodule and subjected to sonoporation treatment as described above. The viable counts were determined by plating serial dilutions onto the blood agar plates. Bacterial survival rate was expressed as the percent ratio of CFU after treatment to CFU before treatment. Each experiment was performed in triplicate and repeated three times.

Statistical analysis. Student's *t* test was employed to compare the bacterial survival rates following different treatments. Differences with P values of <0.05 were considered significant.

RESULTS

Sonoporation is more efficient than electroporation for delivering fluorescent dextran into *F. nucleatum* 12230. To compare the efficiencies of intracellular molecular delivery for sonoporation and electroporation, the same amounts of Texas Red-conjugated dextran (70 kDa) were used for delivery into the same numbers of CFU of *F. nucleatum* 12230. Fluorescence microscopy was used to assess delivery efficiency. Sonoporation was carried out under the conditions previously used to construct the US1 mutant: 0.5-MPa peak positive acoustic pressure, 1-Hz pulse repetition frequency (PRF), 50% duty cycle, and 90 seconds of US exposure duration with a custom-made 1-MHz circular, flat-piston transducer (unfocused) in the presence of 33% (vol/vol) Definity. For controls, sonoporation in the absence of Definity or no sonoporation in the presence of Definity was included. For electroporation, the following conditions were used: 20 kV/cm, 25 μF, and 200 Ω. These were the optimal conditions tested for fusobacteria in different laboratories (5; unpublished results). Efficiency of delivery was expressed as the percentage of fluorescent bacteria compared to the total bacteria enumerated in the same view. For each sample, at least five randomly selected fields were examined, and the average percentage of fluorescent cells was obtained. The survival rate of *F. nucleatum* following treatment was determined by plating serial dilutions of the bacterial suspensions on blood agar plates.

A low level of spontaneous uptake was observed (Fig. 1a), with the background level of fluorescence at approximately 0.4% (Fig. 1b). Delivery of fluorescent dextran into *F. nucleatum* by sonoporation was more efficient than that by electroporation (Fig. 1a). Specifically, delivery by sonoporation in the presence of Definity was at least twice as efficient as that by

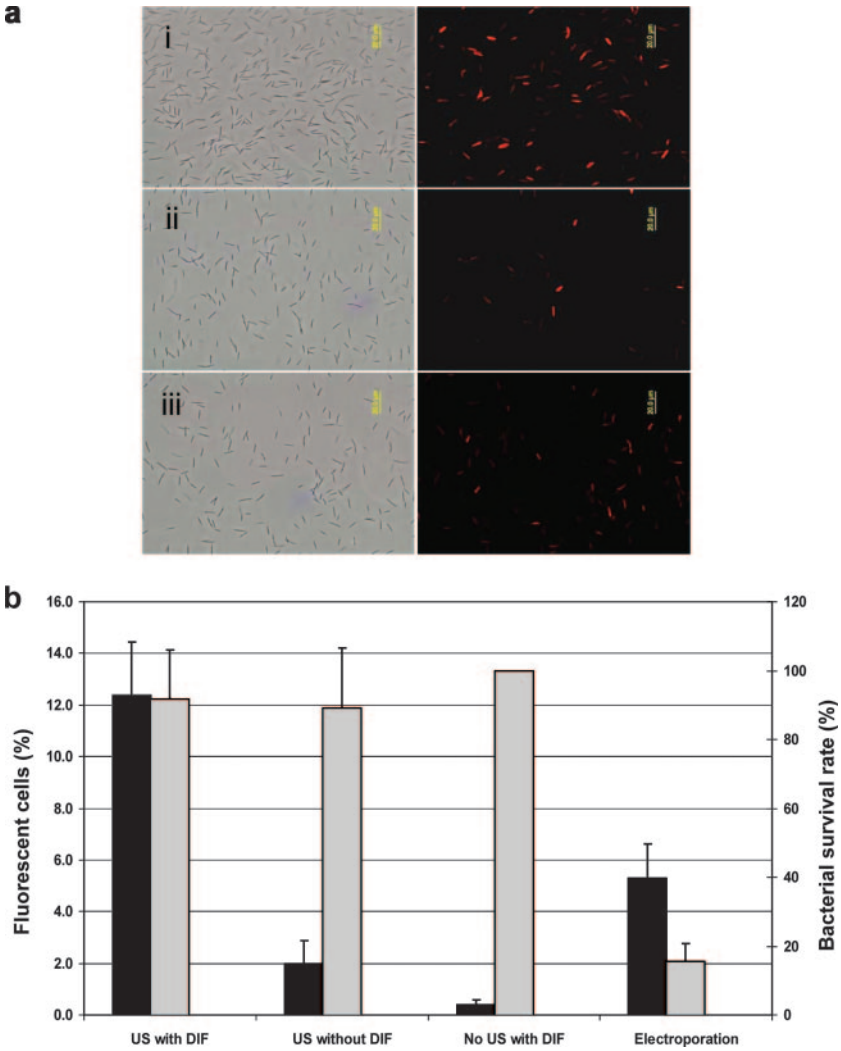

FIG. 1. Delivery of Texas Red-conjugated dextran into *F. nucleatum* 12230 by sonoporation and electroporation. (a) i, fluorescent dextran uptake by *F. nucleatum* 12230 following sonoporation in the presence of Definity; ii, fluorescent dextran uptake by *F. nucleatum* 12230 without US treatment; and iii, fluorescent dextran uptake by *F. nucleatum* 12230 following electroporation. (b) Quantization of fluorescent dextran delivery into *F. nucleatum* 12230 following sonoporation in the presence of Definity, sonoporation in the absence of Definity, no US treatment, and electroporation (black bars, scales on the left). The bacterial survival rate following each treatment is shown with a gray bar (scales on the right). The results shown here are the averages for four individual experiments. The standard deviations are shown above the bars.

electroporation (12.4% versus 5.3%) (Fig. 1b). Sonoporation without Definity resulted in a delivery rate of 2%, suggesting that Definity was required for efficient delivery at the parameters used. Sonoporation under the tested conditions had very little bactericidal effect compared to electroporation, by which >80% of bacteria were killed (Fig. 1b).

The efficiency of fluorescent dextran delivery is affected by multiple parameters of sonoporation. To examine the effects of different parameters on sonoporation in *F. nucleatum*, the rates of fluorescent dextran delivery were compared by varying the value for one parameter while keeping the others constant (Fig. 2). The parameters tested include US pressure amplitude (Fig. 2a), PRF and duty cycle (Fig. 2b), sonoporation duration (Fig. 2c), and quantity of Definity (Fig. 2d). The invariable parameters were set to the same values as those used for Fig. 1. The only exception was the duty cycle value used for Fig. 2a, which was reduced to 5% to allow the testing of amplitudes reaching above 0.9 MPa. Each variable parameter was tested to the maximum allowed by the system. Under our testing conditions, the delivery efficiencies increased with amplitude (Fig. 2a), duty cycle (Fig. 2b), duration of sonoporation (Fig. 2c), and quantity of Definity (Fig. 2d). However, PRF showed no effect (Fig. 2b). The maximum delivery rates obtained for Fig. 2a, b, and d were all between 10 and 15%, and those for Fig. 2c were >20% when the sonoporation duration was increased to 450 s (Fig. 2c). The percentages of viable bacteria following sonoporation were determined; none was significantly different from that for the untreated sample (data not shown). Therefore, sonoporation was nonbactericidal under the testing conditions.

The *recA* gene was conserved in *F. nucleatum* 12230. The *recA* gene with upstream and downstream flanking regions of *F. nucleatum* 12230 was amplified and sequenced using oligonucleotide primers FN0546F and FN0548R. A 1.4-kb PCR

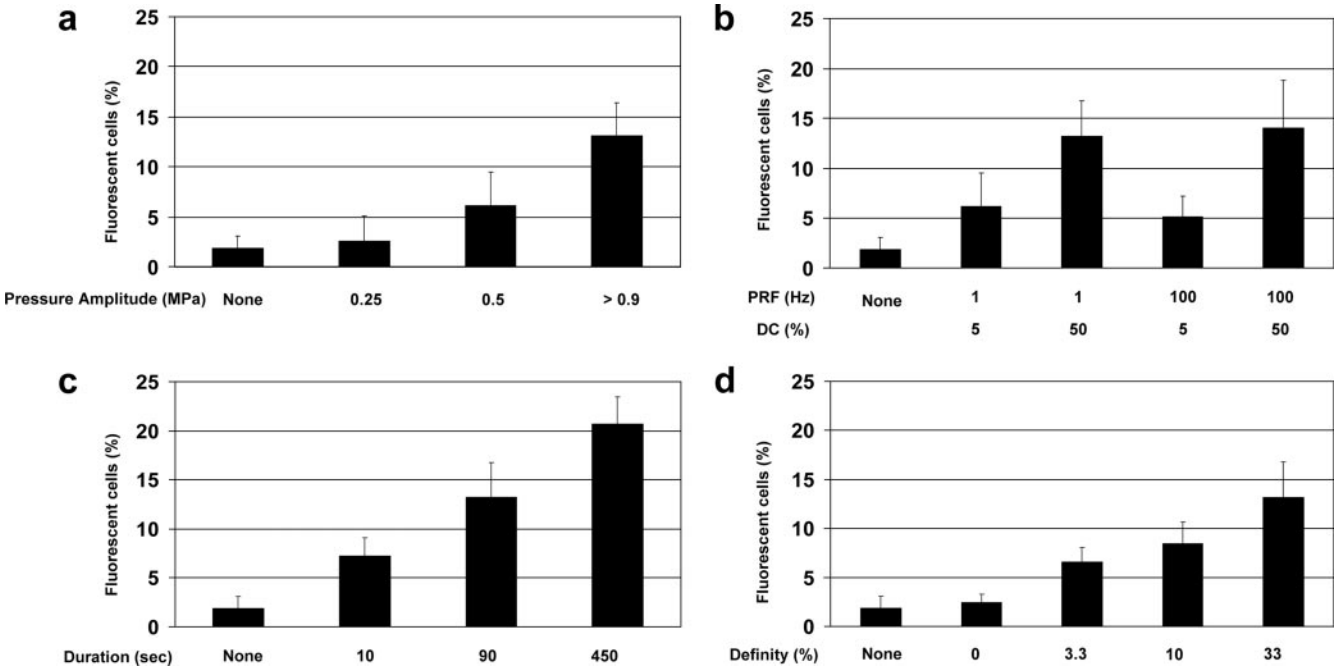

FIG. 2. Effects of different sonoporation parameters, i.e., acoustic pressure amplitude (a), PRF and duty cycle (DC) (b), sonoporation duration (c), and quantity of Definity (d), on delivery of Texas Red-conjugated dextran into *F. nucleatum* 12230. The percentages of fluorescent *F. nucleatum* cells were calculated as follows: percent fluorescent cells = (number of fluorescent cells/total number of cells) × 100. Values are expressed as means and standard deviations (error bars) for three separate experiments performed in triplicate.

fragment containing the 1,140-bp *recA* gene, which encodes 379 amino acid residues with a predicted molecular mass of 40.6 kDa, was obtained. A putative Shine-Dalgarno sequence was identified in the PCR fragment (Fig. 3). The amino acid sequence showed high homologies to the other fusobacterial RecA sequences, with 96% identity to that from *F. nucleatum* ATCC 49256 and 95% identity to that from *F. nucleatum* ATCC 25586 (data not shown). Analysis of the amino acid sequences of RecA from *F. nucleatum* 12230 revealed that it contained 116 out of the 127 RecA consensus residues, with most of the 11 variant residues carrying conserved changes (Fig. 3) (12). The ATP-binding site, i.e., the phosphate-binding loop (P loop), is also conserved in RecA from *F. nucleatum* 12230 (20).

RecA in *F. nucleatum* 12230 was involved in reparable sonoporation. To assess the involvement of RecA in sonoporation, a *recA* mutant in *F. nucleatum* 12230 was constructed. First, a 772-bp N-terminal fragment of the *recA* gene was cloned into vector pCR2.1, followed by insertion of a 2.4-kb *ermF-ermAM* cassette into the HincII site of the cloned fragment, generating pYH1380 (Fig. 4a). The *recA* mutant US1610 was constructed by delivering pYH1380 into *F. nucleatum* 12230 via sonoporation as previously described (7). Clindamycin-resistant clones were isolated at a rate of approximately 0.05 transformants/μg DNA, similar to that for the *fadA* mutant (7). PCR analysis showed that the *ermF-ermAM* cassette was inserted into the *recA* gene on the chromosome by double crossovers (Fig. 4b), also similar to what occurs in the construction of the *fadA* mutant (7). The integrity of pYH1380 was not affected by sonoporation under the testing conditions (Fig. 4c). Therefore, the double-crossover allelic exchange was unlikely due to linearization of the plasmid by sonoporation.

US1610 grew slower than its parental strain both on the blood agar plate and in broth (data not shown), as observed for *recA* mutants of other bacteria (12). As expected, US1610 was significantly more susceptible to UV light (254-nm) irradiation (Fig. 5a), confirming that RecA in *F. nucleatum* 12230 serves a function similar to that which it serves in other microorganisms. Interestingly, US1610 was also more susceptible to US exposure under the sonoporation conditions tested (Fig. 5b) ($P < 0.01$), indicating that sonoporation was bactericidal in the absence of RecA. Thus, RecA played a pivotal role in reparable sonoporation, or survival following US treatment, in *F. nucleatum*.

DISCUSSION

Construction of allelic-exchange mutants is essential to understanding the gene functions. Studies of many organisms have been hindered by a lack of effective genetic tools. *F. nucleatum* is one such example. Conventional approaches, i.e., electroporation, conjugation, and transduction, were unsuccessful in generating desired mutants in most *F. nucleatum* strains, although single-crossover allelic exchange was recently achieved by electroporation in *F. nucleatum* ATCC 23726 (9) and by electroporation and conjugation in *F. nucleatum* 12230, each as an isolated incidence in our laboratory (unpublished results).

F. nucleatum 12230 has been refractory to genetic manipulation. No shuttle plasmid has been delivered into this strain,

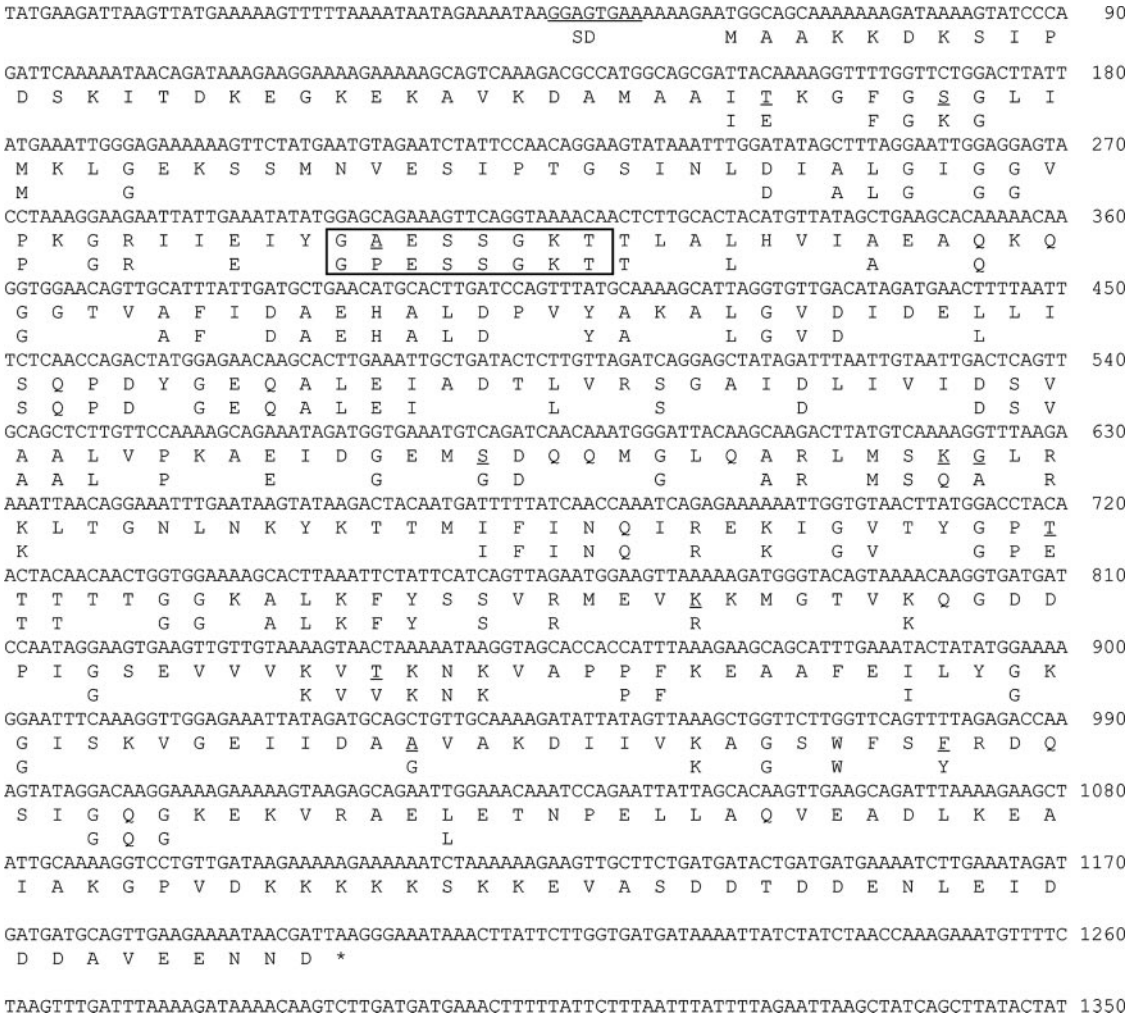

FIG. 3. Nucleotide and deduced amino acid sequences of the *recA* gene of *F. nucleatum* 12230. The putative Shine-Dalgarno sequence (SD) is underlined. The consensus sequence of RecA is listed directly below the amino acid sequence. The 11 residues in *F. nucleatum* 12230 RecA different from those in the consensus sequence are underlined. The P-loop motif (GXXXXGKT) is boxed.

and no gene disruption mutant was generated until the recent construction of US1 by sonoporation. An emerging technology for intracellular molecular delivery, sonoporation was limited to higher eukaryotic cells until recently. Our results demonstrate that, for bacteria with unique features, sonoporation is a versatile delivery and gene transfection tool compared to conventional techniques, such as electroporation. Electroporation transiently reverses membrane potential and impairs cell membrane integrity by forming pores; thus, it mostly delivers negatively charged material, such as DNA. Sonoporation, on the other hand, may have wider applications because it permeabilizes the cell membrane via cavitation, which may be capable of generating larger reversible pores on the membrane, and delivers both charged and noncharged molecules. Furthermore, sonoporation appears to be a "milder" treatment, as most of the bacteria remained alive following treatment, in contrast to electroporation. The high survival rate could increase the efficiency of functional delivery.

Delivery of fluorescent dextran allowed direct quantification of the sonoporation effects (14, 24). Compared to DNA, fluorescent dextran eliminates the complexity associated with nuclease degradation, thus allowing the measurement of delivery only. For the purpose of comparison between sonoporation and electroporation, noncharged fluorescent dextran was chosen for this study because the use of charged fluorescent dextran caused an arc during electroporation (data not shown). It would be interesting to test negatively charged fluorescent dextran, a closer mimic of DNA, in future sonoporation studies.

It has been shown that cavitation is involved in sonoporation and that sonoporation in eukaryotic cells is directly related to bubble-to-cell ratio (23). Although the acoustic pressure threshold of cavitation is not fully understood, several parameters, including the abundance of cavitation nuclei in the exposed medium, affect the process. Microbubble US contrast agents were originally developed and used for US imaging of blood flow, as these micrometer-sized bubbles scatter (interact with) US effectively when injected into the bloodstream, leading to much-improved US imaging capability (1). These gas bubbles enhance sonoporation, most likely by acting as cavita-

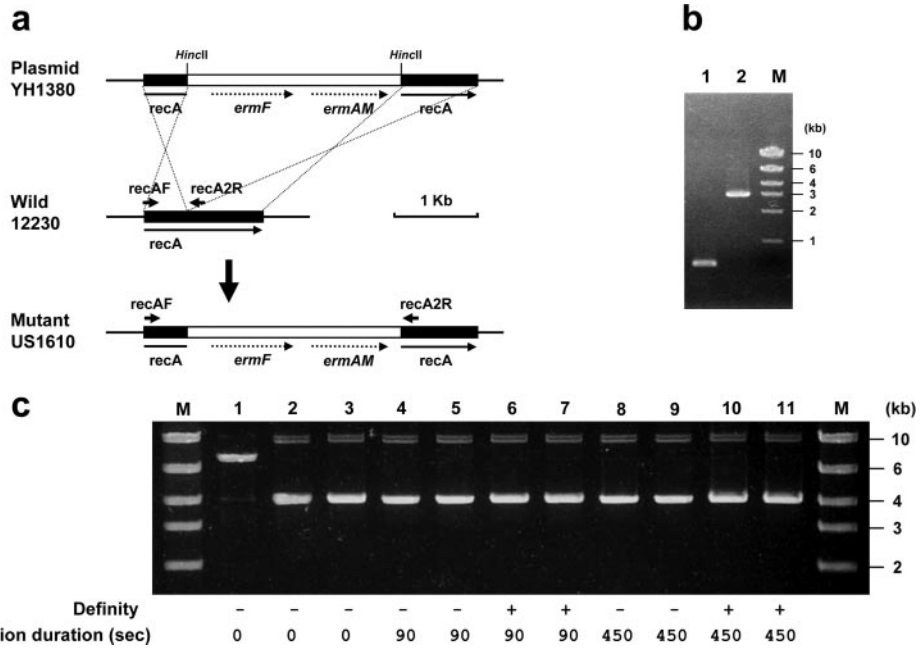

FIG. 4. Construction of the *recA*-defective mutant US1610 of *F. nucleatum* 12230. (a) Schematic representation of the construction of the *recA*::*ermF-ermAM* mutant. The *ermF-ermAM* cassette was inserted at the HincII site in *recA*, conferring clindamycin resistance. (b) PCR analysis of *F. nucleatum* 12230 and US1610 chromosomes using primers *recA*F and *recA*2R. Lane 1, *F. nucleatum* 12230; lane 2, US1610. M, molecular size makers as indicated on the right. (c) Effects of different sonoporation conditions on the integrity of pYH1380. Lane 1, linearized pYH1380 following EcoRV digestion; lane 2, untreated intact pYH1380; lane 3, untreated intact pYH1380 in the presence of Definity; lanes 4, 5, 8, and 9, pYH1380 treated with sonoporation in the absence of Definity; lanes 6, 7, 10, and 11, pYH1380 treated with sonoporation in the presence of Definity. M, DNA molecular size markers. The sonoporation durations and the presence (+) or absence (−) of Definity are indicated below the gel. Each condition was tested in duplicate.

tion nuclei and decreasing the cavitation threshold. Definity, a commercially available contrast agent consisting of lipid-covered microspheres filled with octafluoropropane, was used in this study. The *recA* mutant was obtained at a frequency of 0.05 transformants/μg DNA, similar to that for the *fadA* deletion mutant, which was generated using Optison (perflutren protein type A microspheres for injection; USP, Amersham, Princeton, NJ), consisting of albumin-covered microspheres filled with octafluoropropane. Two contrast agents, differing in bubble size, chemical component content, and stock concentration, allowed for production of different mutants at similar frequencies. This confirms that the contrast agent bubbles served as cavitation nuclei and facilitated sonoporation physically. It is likely that delivery efficiency reached a plateau under the sonoporation conditions used in this study for mutant construction.

Besides bubble-to-cell ratio, other factors affecting sonoporation in eukaryotic cells include acoustic pressure amplitude, duty cycle, PRF, and exposure time (2, 14, 18, 24). Among these, increases of acoustic pressure amplitude, duty cycle, and exposure time had similar effects on sonoporation in *F. nucleatum*. Sonoporation efficiency improved with increased values for acoustic pressure amplitude, duty cycle, and exposure time, which were all tested to the maximum capacities allowed by the transducer used. A new transducer allowing further enhancement of these parameters is currently under testing. Under our testing conditions, PRF had no effect on bacterial sonoporation.

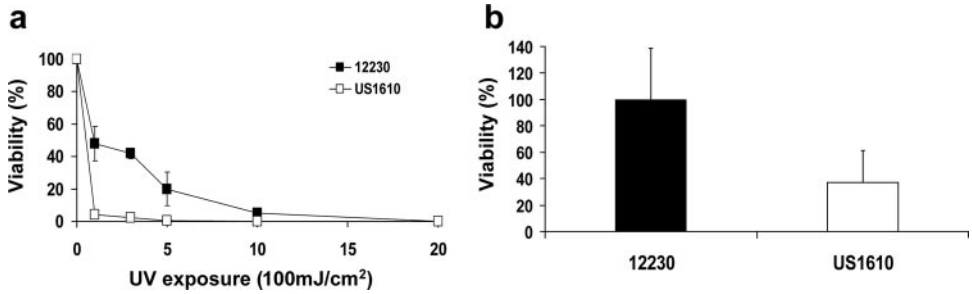

FIG. 5. Susceptibilities of *F. nucleatum* 12230 and US1610 to UV (a) and sonoporation (b). Percent bacterial viability was expressed as the number of CFU following treatment over the total number of CFU prior to treatment. The sonoporation conditions used were 0.5 MPa, 1-Hz PRF, 90-s duration, 50% duty cycle, and 33% Definity (vol/vol). The standard deviations are indicated above and below the squares (a) or above the bars (b).

One striking resemblance and notable feature shared by the construction of US1 and US1610 by sonoporation was that both were obtained through one-step double-crossover allelic exchanges. One-step double crossovers are highly unlikely events under conventional conditions, such as electroporation and conjugation. However, as has been observed consistently in two different mutants, the one-step double crossover was most likely a unique feature of gene transfection by sonoporation in bacteria, differing from that in eukaryotic cells, which normally leads to random insertion of the plasmid. It also differs from electroporation in bacteria, which generates single crossovers, resulting in insertion of the entire plasmid. To obtain double crossovers using intact plasmids would normally involve a second step for selection for the loss of the integrated plasmid. If the suicide plasmid contains an internal fragment of the targeted gene, integration of the plasmid into the chromosome generates an insertional mutation. This mutation is unstable, as the plasmid may "loop" out of the chromosome, leading to loss of the mutation. To achieve one-step double-crossover mutation by electroporation, the plasmid needs to be linearized, which renders the electroporation inefficient. The unique features of one-step double crossovers obtained using intact plasmids signify sonoporation as a potentially powerful genetic tool for streamlining mutant construction.

The increased double-crossover frequencies in the absence of linearization of the suicide plasmids led to the speculation that sonoporation might have activated the recombination machinery. Therefore, the *recA* mutant US1610 was constructed to ascertain its involvement. The mutant was susceptible to UV exposure compared to its wild-type parental strain, indicating that the RecA function was conserved in *F. nucleatum*. Interestingly, US1610 was also more susceptible to US exposure, suggesting that RecA was involved in helping the cells recover from the damages caused by sonoporation. Sonoporation may activate the stress response genes, including RecA, thus increasing the frequency of double-crossover homologous recombination. Although no structural damage was observed for the suicide plasmids, it may be possible that nicking of the much longer bacterial chromosomal DNA occurred during sonoporation.

In summary, gene transfection by sonoporation in bacteria differs from that in eukaryotic cells, leading to targeted gene disruption. This technology also differs from electroporation in several aspects: (i) it is more efficient for intracellular delivery, (ii) it is nonbactericidal under tested conditions, and (iii) it leads to one-step double-crossover allelic exchanges. RecA was identified to be involved in reparable sonoporation, which may stimulate the SOS response, thus enhancing the homologous recombination activities inside the cells and leading to double-crossover allelic exchanges. Sonoporation implies tremendous potential for streamlining mutant construction in bacteria.

ACKNOWLEDGMENTS

This work was supported in part by NIH grant RO1 DE 14924 and a Philip Morris External Research fund to Y.W.H. and NIH grant RO1 CA116592 to C.X.D.

REFERENCES

1. **Deng, C. X., and F. L. Lizzi.** 2002. A review of physical phenomena associated with ultrasonic contrast agents and illustrative clinical applications. Ultrasound Med. Biol. **28:**277–286.
2. **Deng, C. X., F. Sieling, H. Pan, and J. Cui.** 2004. Ultrasound-induced cell membrane porosity. Ultrasound Med. Biol. **30:**519–526.
3. **Fenno, J. C., A. Shaikh, and P. Fives-Taylor.** 1993. Characterization of allelic replacement in Streptococcus parasanguis: transformation and homologous recombination in a 'nontransformable' streptococcus. Gene **130:**81–90.
4. **Fletcher, H. M., H. A. Schenkein, R. M. Morgan, K. A. Bailey, C. R. Berry, and F. L. Macrina.** 1995. Virulence of a *Porphyromonas gingivalis* W83 mutant defective in the *prtH* gene. Infect. Immun. **63:**1521–1528.
5. **Haake, S. K., S. C. Yoder, G. Attarian, and K. Podkaminer.** 2000. Native plasmids of *Fusobacterium nucleatum*: characterization and use in development of genetic systems. J. Bacteriol. **182:**1176–1180.
6. **Han, Y. W.** 2006. Laboratory maintenance of fusobacteria, unit 13A. *In* T. K. R. Coico, J. Quarles, B. Stevenson, and R. Taylor (ed.), Current protocols in microbiology. John Wiley & Sons, Inc., New York, NY.
7. **Han, Y. W., A. Ikegami, C. Rajanna, H. I. Kawsar, Y. Zhou, M. Li, H. T. Sojar, R. J. Genco, H. K. Kuramitsu, and C. X. Deng.** 2005. Identification and characterization of a novel adhesin unique to oral fusobacteria. J. Bacteriol. **187:**5330–5340.
8. **Inagaki, H., J. Suzuki, M. Ogawa, Y. Taniyama, R. Morishita, and M. Isobe.** 2006. Ultrasound-microbubble-mediated NF-kappaB decoy transfection attenuates neointimal formation after arterial injury in mice. J. Vasc. Res. **43:**12–18.
9. **Kaplan, C. W., R. Lux, T. Huynh, A. Jewett, W. Shi, and S. K. Haake.** 2005. Fusobacterium nucleatum apoptosis-inducing outer membrane protein. J. Dent. Res. **84:**700–704.
10. **Kinder Haake, S., S. Yoder, and S. H. Gerardo.** 2006. Efficient gene transfer and targeted mutagenesis in Fusobacterium nucleatum. Plasmid **55:**27–38.

10a. **Liu, Z., N. Guiliani, C. Appia-Ayme, F. Borne, J. Ratouchniak, and V. Bonnefoy.** 2000. Construction and characterization of a *recA* mutant of *Thiobacillus ferroxidans* by marker exchange mutagenesis. J. Bacteriol. **182:**2269–2276.

11. **Lui, A., B. C. McBride, G. F. Vovis, and M. Smith.** 1979. Site specific endonuclease from Fusobacterium nucleatum. Nucleic Acids Res. **6:**1–15.
12. **Lusetti, S. L., and M. M. Cox.** 2002. The bacterial RecA protein and the recombinational DNA repair of stalled replication forks. Annu. Rev. Biochem. **71:**71–100.
13. **McKay, T. L., J. Ko, Y. Bilalis, and J. M. DiRienzo.** 1995. Mobile genetic elements of Fusobacterium nucleatum. Plasmid **33:**15–25.
14. **Miller, D. L., S. V. Pislaru, and J. E. Greenleaf.** 2002. Sonoporation: mechanical DNA delivery by ultrasonic cavitation. Somat. Cell Mol. Genet. **27:**115–134.
15. **Miyake, T., M. Aoki, H. Nakashima, T. Kawasaki, M. Oishi, K. Kataoka, K. Tanemoto, T. Ogihara, Y. Kaneda, and R. Morishita.** 2006. Prevention of abdominal aortic aneurysms by simultaneous inhibition of NFkappaB and ets using chimeric decoy oligonucleotides in a rabbit model. Gene Ther. **13:**695–704.
16. **Moore, W. E., and L. V. Moore.** 1994. The bacteria of periodontal diseases. Periodontol. 2000 **5:**66–77.
17. **Muller, O. J., H. A. Katus, and R. Bekeredjian.** 2007. Targeting the heart with gene therapy-optimized gene delivery methods. Cardiovasc. Res. **73:**453–462.
18. **Pan, H., Y. Zhou, O. Izadnegahdar, J. Cui, and C. X. Deng.** 2005. Study of sonoporation dynamics affected by ultrasound duty cycle. Ultrasound Med. Biol. **31:**849–856.
19. **Pozzi, G., and W. R. Guild.** 1985. Modes of integration of heterologous plasmid DNA into the chromosome of *Streptococcus pneumoniae*. J. Bacteriol. **161:**909–912.
20. **Saraste, M., P. R. Sibbald, and A. Wittinghofer.** 1990. The P-loop—a common motif in ATP- and GTP-binding proteins. Trends Biochem. Sci. **15:**430–434.
21. **Shimamura, M., N. Sato, Y. Taniyama, S. Yamamoto, M. Endoh, H. Kurinami, M. Aoki, T. Ogihara, Y. Kaneda, and R. Morishita.** 2004. Development of efficient plasmid DNA transfer into adult rat central nervous system using microbubble-enhanced ultrasound. Gene Ther. **11:**1532–1539.
22. **Takahashi, M., K. Kido, A. Aoi, H. Furukawa, M. Ono, and T. Kodama.** 2007. Spinal gene transfer using ultrasound and microbubbles. J. Control Release **117:**267–272.
23. **Ward, M., J. Wu, and J. F. Chiu.** 2000. Experimental study of the effects of Optison concentration on sonoporation in vitro. Ultrasound Med. Biol. **26:**1169–1175.
24. **Zarnitsyn, V. G., and M. R. Prausnitz.** 2004. Physical parameters influencing optimization of ultrasound-mediated DNA transfection. Ultrasound Med. Biol. **30:**527–538.